

Deep BOO: Automating Beam Orientation Optimization in Intensity Modulated Radiation Therapy.

Olalekan Ogunmolu*, Michael Folkerts*, Dan Nguyen*, Nicholas Gans[†], and Steve Jiang*

*Department of Radiation Oncology, UT Southwestern Medical Center,
2280 Inwood Road, Dallas, Texas 75390-9303, USA

[†]Department of Electrical Engineering, University of Texas at Dallas,
Richardson, TX 75080, USA

{olalekan.ogunmolu, steve.jiang}@utsouthwestern.edu
michael.folkerts@varian.com, ngans@utdallas.edu

Abstract. Finding the right beam angle set from a robot’s tool frame from which to maximally aim radiation to cancer tumor(s) while minimizing radiation to sensitive organs during intensity modulated radiation therapy (IMRT) is an exhaustive combinatorial search or set-cover problem and traditional optimization methods have not yielded real-time feasible results. Aiming to automate the beam orientation and intensity modulation process, we introduce a novel set of techniques leveraging on (i) pattern recognition. In this sentiment, we optimize a deep neural network policy which guides monte carlo simulations of promising beamlets. Seeking a saddle equilibrium, we let two fictitious neural network players, within a zero-sum markov game framework, alternately play a best response to their opponent’s mixed strategy profile during episodes of a markov decision process. At inference time, we run the trained policy on test patients’ target volumes to predict feasible beam angles. This work merges the beam orientation and fluence map optimization subproblems in IMRT sequential treatment planning system into one pipeline. We formally introduce our approach, and present numerical simulation results for coplanar beam angles on prostate cases.

1 Introduction

Intensity Modulated Radiation Therapy (IMRT) is a state-of-the-art cancer treatment method that delivers high-precision x-rays or electron beams by modulating the intensity of the radiation beam from a robot’s eye-view, and modifying the geometric field-shape of the resultant beam in order to produce conformal dose distributions around a tumor, typically located in a patient lying in a supine position on a linear accelerator (LINAC) table. Before treatment, a doctor contours the *critical structures* (or tumors) and *organs-at-risk* (or OARs) within a *target volume* (region of the patient’s computed tomography (CT) or magnetic resonance (MRI) scan that contains the tumor and other organs), then prescribes doses that must be delivered. Each beam to be delivered consists of beamlets, aimed from the same angle, where each beamlet may be of a different intensity from that of its neighbors. Generally, the radiation intensities are delivered from about 5 ~ 11 different beam orientations with multiple collimator units. The process of choosing

what beam angle is best for delivering beamlet intensities is termed *beam orientation optimization* (BOO) while the process of determining what intensity meets a prescribed fluence profile by a doctor is termed *fluence map optimization* (FMO).

A good radiation profile “influence” should simultaneously maximize and minimize the dose delivered to tumor(s) and OARs respectively, while producing sharp dose gradients at the transition between tumors and OARs. This problem has a conflicted objective because tumor(s) often intersect(s) with OARs, and the dose deposition’s physics changes with each beam orientation so that the BOO is a non-convex problem [1], [2] with myriads of possible beam combinations within a robot’s phase space. As such, finding good candidate beam angles in practice is a trial-and-error search process, with success depending on the treatment planner’s experience and the amount of time spent on tuning the angles. Selecting beams by trial-and-error is laden with the subjectivity of the treatment planner (TP), and the time taken to find good candidate beam angles set is often not real-time feasible.

Mathematically, this can be seen as a set cover problem, where given a universe of all candidate beam angles, \mathcal{U} , we seek to find from a family \mathcal{S} of subsets of \mathcal{U} , a cover subfamily, $\mathcal{C} \subseteq \mathcal{S}$ whose union is an optimal beam set that meets the doctor’s prescription. This is a combinatorics problem where the dimensionality of the parameters to be optimized increases to the extent that classical optimization methods are not real-time feasible. When just the gantry (the robot’s tool frame) is rotated with respect to the pose of the patient, we have *coplanar beams*, *i.e.* all other joint angles of the robot are fixed while only the head rotates – resulting in a set of coplanar beams that are swept out by the gantry. In this paper, we focus on finding good coplanar beams in BOO problems as more often than not, only coplanar beams are employed when delivering radiation [3]. We resort to an approximate dynamic programming (ADP) formulation to derive *approximately optimal policies* in high dimensional state spaces. Particularly, we leverage on recent machine learning breakthroughs [4] to guide a Monte Carlo Tree Search (MCTS) [5–7] of promising beam angle candidates by rapidly exploring different parts of the beam space. We reckon that having an automated toolset for choosing desirable beam angles will eradicate the manual search process, and save treatment time.



IMRT TPS setup. ©radiologyinfo.org

1.1 Contributions

We provide pseudocode that transforms the BOO problem into a game planning strategy. Coupled with neural fictitious self-play, we continually refine the predictions from a neural network policy so as to drive the weights of the network to a **saddle equilibrium** [8]. To this end,

- we let a deep neural network model the nonlinear dynamical system and we generate policies that guide MCTS simulations for two players in a zero-sum Markov game

- an MCTS tree lookout strategy guides transition from one beam angle set to another during each markov decision process (MDP) setting for either player
- each player finds a best response strategy to its opponent’s average strategy – driving the weights of the network policy toward an approximate **saddle equilibrium** [9]

Note that in contrast to simulated annealing approaches, our approach takes a very complicated nonlinear problem, solves it offline, saves the weights of the neural network, and then at test time, uses the saved weights to predict feasible beam angles. This is the first article, to the best of our knowledge, that provides a comprehensive description of MCTS within the framework of the classic BOO problem.

1.2 Related Work

Mathematical formulations for choosing feasible beam angles from which a good clinical plan can be achieved range from deterministic optimization to stochastic optimization approaches. Craft [1] locally tuned a beam angle set within a beam’s continuous state space using linear programming duality theory and gradient descent, and found that the BOO problem for a simple 2D pancreatic case has ≈ 100 minima when local optimization is warm-started from 100 different beam angles. Building on Craft’s work, Bertsimas et. al [10] resolved to a two meta-step algorithm: dynamically selecting beam angle candidates within the continuous beams’ phase space via local minimum search with gradient descent, then exploring a different portion of the solution space by taking finite steps of simulated annealing. Bertsimas et. al [10] defined a linear programming problem with constraints that capture a doctor’s preference for dose delivery. While this approach takes advantage of global and local search with improvements in solutions obtained from equispaced angles, it has the drawback of presenting the objective function as convex and assuming the doctor’s preferences can be represented as a set of linear constraints.

Jia et. al [11] split the BOO problem into two consecutive phases: first, by progressively identifying non-consequential beam angles through the evaluation of a multi objective function, and secondly, by optimizing the fluence on beam angles that are assigned a high confidence by a dosimetric objective component. Heuristic search strategies have also previously developed e.g. [12–14]. Other lines of work have treated IMRT treatment planning as an inverse optimization problem, with techniques ranging from adaptive l_{21} optimization [11], mixed integer linear programming [15–17] and simulated annealing [3, 18].

2 Methods and Materials

Our design philosophy draws inspiration from approximate dynamic programming, optimal control theory, and game theory. For games with perfect information, there is an optimal value function, $v^*(s)$, that decides the game’s outcome for every possible state under perfect play. It follows that one can devise a planning strategy that guides the search for optimistic beam angle configurations within the beam phase space by using a probability distribution, $p(s, a)$, over a set of deterministic *pure strategies* for the tree [9].

2.1 Overview

The search for an *approximately* optimal beam angle set is performed by optimizing the parameters of a function approximator, ψ , which approximate a policy, π . MCTS simulations of ‘best-first’ beam angle combinations are guided by π for a sufficient number of iterations; our MCTS performs a sparse lookout simulation, recursively expanding sub-nodes the tree’s root node, and selectively adjusting the beam angle(s) that contribute the least to an optimal fluence within a node’s beam set. Successor nodes beneath a terminal node are **approximated** with a value, $v(s)$, to assure efficient selectivity.

We model the decision process for optimal beam selection by maintaining a probability distribution over possible states, based on a set of observations and observation probabilities for the underlying MDP. The policy that guides the search for the optimal beam angle selection is computed by a deep neural network policy, consisting of multiple residual blocks fashioned similar to modern neural network architectures [19, 20]. First, let us formalize definitions and notations used throughout the rest of this document.

2.2 Notations and Definitions

The state of the dynamical system, will be denoted by $s \in \mathcal{S}$, and it is to be controlled by a discrete action $a \in \mathcal{A}$. States evolve according to the (unknown) dynamics $p(s_{t+1}|s_t, a_t)$, which we want to learn. We pose the learning problem within a discrete-time finite-time horizon, T . A beam angle combination search task in this setting can be defined by a reward function $r(s_t, a_t)$, that can be found by recovering a policy $p(a_t|s_t; \psi)$ which specifies a distribution over actions conditioned on the state and parameterized by some vector ψ . The parameters, ψ , might correspond to the weights of a neural network for example. Without loss of generality, we will denote the action conditional $p(a_t|s_t, \psi)$ as $\pi_\psi(a_t|s_t)$. Recovering the optimal weights may consist of the maximization problem,

$$\psi^* = \arg \max_{\psi} \sum_{t=1}^T \mathbb{E}_{(s_t, a_t) \sim p(s_t, a_t | \psi)} [r(s_t, a_t)],$$

where the we seek to determine an optimal neural network weight matrix ψ^* that maximize the sum of the respective instantaneous rewards $\sum_t r(s_t, a_t)$ of the policy, $\pi_\psi(a_t|s_t)$. Let us now introduce some definitions.

Definition 1. A *beam block* is a concatenation of beams, $\{\theta_1, \theta_2, \dots, \theta_m\}$ as a tensor of dimension $m \times C \times H \times W$ (see Fig. 2) that together with the patient’s ct mask form the state, s_t , at time step, t .

In order for the state definition to capture as much information as possible under uncertainty, we define the state broadly enough to capture all subjective unknowns that might influence the payoff/reward to be received by a rational decision-making agent. We want an adaptive allocation rule for determining the transition between states such that as the search process progresses, and achieves convergence as the simulation grows, the worst possible bias is bounded by a quantity that converges to zero. We leverage on the *upper confidence bound* algorithm of Agrawal [21] that assures an asymptotic

logarithmic regret behavior. Since we do not know what node may yield the best bandit, a player might be biased towards always selecting the beams set with the maximum value. Therefore, we attach a regret term, $U(n(s))$ to the $Q(s, a)$ -value so as to ensure the optimal beam does not evade the simulation *i.e.* $Q(s, a) - U(n(s)) \leq Q(s, a) \leq Q(s, a) + U(n(s))$; the width of this confidence bound guides the exploration strategy for states that are momentarily unpromising in values but may later emerge as promising states as the number of games evolve in length.

Definition 2. Every **node** of the tree, \mathbf{x} , has the following fields: (i) a pointer to the parent that led to it, $\mathbf{x}.p$; (ii) the beamlets, \mathbf{x}_b , stored at that node where $b = \{1, \dots, m\}$; (iii) a set of move probabilities prior, $p(s, a)$; (iv) a pointer, $\mathbf{x}.r$, to the reward, r_t , for the state s_t ; (v) a pointer to the state-action value $Q(s, a)$ and its upper confidence bound

Notation	Definition/Examples	Notation	Definition/Examples
m	dimensionality of a node's beam set, e.g. $m = 5$	n	dimension of discretized beam angles, e.g. $n = 180$ for 4° angular resolution
Θ	discretized beam angle set e.g. equally spaced angles between 0° and 360° , spaced apart at 4°	$a_t \in \mathcal{A}$	control or action, $a_t \in \mathcal{A}$ at time step $t \in [1, T]$ used in determining the probability of transitioning from a beam angle subset to another within Θ
$\theta^j \subseteq \Theta$	beam angles selected from Θ e.g. $\theta_k \in \mathbb{R}^m$	$s_t \in \mathcal{S}$	markovian system state at time step, $t \in [1, T]$ e.g. patient contour, beam angle candidates; dimensionality 2, 727, 936 to 3, 563, 520
γ	discount factor e.g. 0.99	f_ψ	parametric function approximator (deep neural network policy) for state s_t
$v_\psi(s)$	value estimate of state, s_t , as predicted by f_ψ	$p(s)$	probability distribution over current state, s generated by neural network policy
$Q(s, a)$	action-state values that encode the "goodness" of a beam-angle set, $\theta_k \in \mathbb{R}^m$, where m is the number of beams considered for a fluence generation, e.g. $m = 5$	\mathbf{B}_{X_t}	a concatenation of beams in consideration at time step, t , as a block of beams being fed to the neural network policy
$\mathcal{D}_{ij}(\theta_k)$	dose matrix containing dose influence to voxel i from beam angle, θ_k , $\forall k \in \{1, 2, \dots, n\}$ where n is range of the beam set \mathcal{B}	\mathbf{D}_t	dose mask for target volume in consideration at time step, t

Table 1: Table of notations commonly used in this article

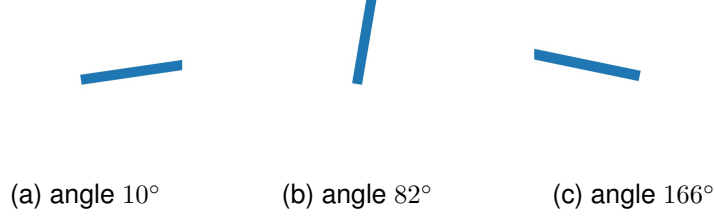


Fig. 1: Example 2D gantry angle representations

$U(s, a)$ (6) (vi) a visit count, $N(s, a)$, that indicates the number of times that node was visited; and (vii) a pointer $x.child_i$ to each of its children nodes.

Other notations used in the article are delineated in Table 1.

2.3 Data Preprocessing

Here, we describe masks preprocessing before training the network.

Patient Mask. We obtained 77 anonymized patient CT scans and associated data from our clinic. The scans relate to prostate cases used in previous IMRT cancer TP. The prostate data contains scans of six organs, namely the patients’ body, bladder, left and right femoral heads, rectum, and planning target volume (PTV) or tumor. Each patient’s scan, D , is represented in 3D as $N \times W \times H$, where N is the total number of slices, W is the slice width and H is the slice height. We resized each slice to a square-shaped 2D matrix of size 64×64 . We generate 3D images that represent the orientation of the gantry with respect to the patient for each discretized beam angle as shown in (Fig. 1).

2.4 Neural Network Architecture

In addition to the resized masks, D , we define five feature planes, X_t as a block of beam configurations: B_{X_t} , denotes the beam angles that generate the current fluence. For example, if we are considering five beams for the geometric shape for the fluence, B_{X_t} would contain the 3D RGB images of the beams being considered at time step t . We then augment the state with a memory of five previously used beam blocks, $\{B_{X_t}, \dots, B_{X_{t-5}}\}$, during the search process; we make this augmentation due to the partial observability of the patient-gantry setup from a single set of features, in order to mitigate the uncertainty of decisions under our partially observable MDP formulation.

The dose masks and beam blocks are as shown in Fig. 2 so that the input planes to the network are sized as $T \times N \times H \times W$ where T is the total number of input planes ($T = 6 \text{ structures} + 5 \text{ beams} + 5 \times 5 \text{ regressed beams} = 36$). Thus, the input to the network are arranged as: $s_t = [D_t, B_{X_t}, B_{X_{t-1}}, B_{X_{t-2}}, B_{X_{t-3}}, B_{X_{t-4}}, B_{X_{t-5}}]$. To address robust learning of patient geometry and beam angle orientations, we use a modern neural network architecture with many residual blocks [20] so that each layer of the network fits a residual nonlinear mapping to its input data; we end up with a deeply stacked network whose input features, s_t , are processed by 34 residual blocks described as

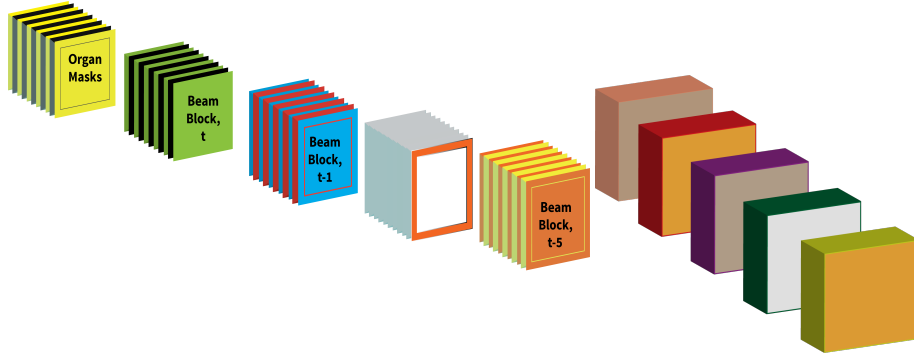


Fig. 2: [Left]: Concatenation of the target volume masks and the beam angles before feeding the input planes to the residual tower neural network. The first six planes (top-most mask of left figure) contain the delineated organs and the PTV. This is concatenated with a block of m beams from the current time step, regressed to the previous 5 time steps (here, 5 was heuristically chosen). [Right] Each beam angle in a beam block is represented as shown. Together with the target volume, these form an input plane of size $36 \times N \times W \times H$ to the policy/value neural network tower of residual blocks.

follows: (i) a 3D convolution with $64 \times l$ filters, a square kernel of width 7, and double strided convolutions, where l is the depth of the stack in the network; (ii) a 3D batch normalization layer [22]; (iii) nonlinear rectifiers [23]; (iv) a 3D convolution of $64 \times l$ filters; (v) a 3D batch normalization layer; (vi) a skip connection from the input to the block, in order to facilitate efficient gradients' propagation; and (vii) nonlinear rectifiers.

We split the output of the network into two heads: (i) the first head is a probability distribution over which angle in the current beam block contributes the least to an optimal fluence cost at the current time step, while (ii) the second head estimates the *value* (in an *ADP sense*) of the subtree beneath the current node. This probability head is comprised of two residual blocks, each containing: (i) a 3D convolution of $64 \times l$ filters, followed by a square kernel of size 1, and a single strided convolution; (ii) a 3D batch normalization layer; (iii) nonlinear rectifiers; (iv) a 3D convolution of $64 \times l$ filters; (v) a 3D batch normalization layer; (vi) a skip connection from the input to the block; (vii) nonlinear rectifiers; (viii) a fully connected layer that maps the resulting output to the total number of discretized beam angle grids; and (ix) a softmax layer then maps the neuron units to logit probabilities $p_i(s|a)$ for all beam angles.

The value head applies the following transformation modules (i) a 3D convolution of $64 \times l$ filters, a square kernel of size 1, and a single strided convolution; (ii) a 3D batch normalization layer; (iii) nonlinear rectifiers; (iv) a second 3D convolution of $64 \times l$ filters; (v) a 3D batch normalization layer; (vi) a skip connection from the input to the block; (vii) nonlinear rectifiers and a sequential layer consisting of:

- a linear layer that maps the output of the above connections to a 512-layer hidden unit
- a linear layer that maps the output of the above connections to a 256 hidden unit followed by rectified nonlinearities

- a linear layer that maps to a scalar value, and followed by rectified nonlinearities
- a tanh nonlinearity that maps the output to the closed interval $[-1, 1]$.

The parameters of the neural network were initialized using the initialization method proposed in [24]. The value and the probability distribution heads are inspired from Bayesian decision theory, whereby it is expected that a rational decision-maker’s behavior is describable by a *utility function*, (or value function) – a quantitative characterization of the policy’s preferences for an outcome – and a subjective probability distribution, which describes the policy’s beliefs about all relevant unknown factors. When new information is presented to the decision-maker, the subjective probability distribution should be revised. Since decisions about what beam angle combination is optimal at the current time step are made under uncertainty, we use a *probability model* to choose among **lotteries**, where the lotteries in this case are probability distributions over all discretized beam angles in our setting. Each state during our learning process is constructed by appending the beam block at the current time step to a history of beam blocks for the previous five time steps using a FIFO policy. Specifically, when we transition to a new state, the beam block that has been in the state set for the longest time (*i.e.* at the **head** of the queue) is deleted first, and the new state’s beam block is enqueued at the tail as in a **queue** data structure. This is so as to minimize the partial observability of the system.

2.5 Fluence Map Optimization

Suppose \mathcal{X} is the total number of discretized voxels of interest (*VOI*’s) in a target volume, and $\mathcal{B}_1 \cup \mathcal{B}_2 \cup \dots \cup \mathcal{B}_n \subseteq \mathcal{B}$ represents the partition subset of a beam \mathcal{B} , where n is the total number of beams from which radiation can be delivered. Suppose we let $\mathcal{D}_{ij}(\theta_k)$ be the matrix that describes each dose influence, d_i , delivered to a discretized voxel, i , in a volume of interest, VOI_h ($h = 1, \dots, \mathcal{X}$), from a beam angle, θ_k , $k \in \{1, \dots, n\}$, then it follows that one can compute the matrix $\mathcal{D}_{ij}(\theta_k)$ by calculating each d_i for every bixel, j , at every φ° , $j \in \mathcal{B}_k$ resolution. Doing this, we end up with a large but sparse matrix, $\mathcal{D}_{ij}(\theta_k)$, which consists of the dose to every voxel, i , incident from a beam angle, θ_k at every $360^\circ/\varphi^\circ$ (in our implementation, we set φ to 4°).

For a decision variable, x_j , representing the intensities of beamlets, $j \in \mathcal{B}$, it is trivial to find the dose influence, d_i , that relates the bixel intensities, x_j , to the voxels of interest, VOI_h . The fluence problem aims to find the values of x_j for which the d_i to the tumor is maximized, while simultaneously minimizing the d_i to critical structures. These objectives are conflicting by definition, and it is typical for dosimetrists to spend hours finding a good set of candidate beams. For the voxels in all OARs, a weighted quadratic objective minimizes the l_2 distance between a pre-calculated dose \mathbf{Ax} , and a doctor’s prescribed dose, \mathbf{b} , while a weighted quadratic objective maximizes the l_2 distance between \mathbf{Ax} and \mathbf{b} . The pre-calculated dose term is given by $\mathbf{Ax} = \{\sum_s \frac{w_s}{v_s} \mathcal{D}_{ij}^s \mathbf{x}_s \mid \mathcal{D}_{ij} \in \mathbb{R}^{n \times l}, n > l\}$, which is a combination of the dose components that belong to OARs and those that belong to PTVs. $w_s = \{\underline{w}_s, \bar{w}_s\}$ are the respective underdosing and overdosing weights for the OARs and PTVs, and v_s represents the total number of voxels

in each structure. The cost function is

$$\frac{1}{v_s} \sum_{s \in \text{OARs}} \|(b_s - \underline{w}_s \mathcal{D}_{ij}^s \mathbf{x}_s)_+\|_2^2 + \frac{1}{v_s} \sum_{s \in \text{PTVs}} \|(\bar{w}_s \mathcal{D}_{ij}^s \mathbf{x}_s - b_s)_+\|_2^2 \quad (1)$$

where the underdosing weights are typically set as $\underline{w}_s = 0$ since it is desirable to deliver as little dose as possible to critical structures, while the overdosing weights are chosen to deliver the prescribed dose to the tumor; $(\cdot)_+$ denotes a Euclidean projection onto the nonnegative orthant \mathbb{R}_+ . We can succinctly write the above objective function, subject to nonnegative bixel intensity constraints, as

$$\min \frac{1}{2} \|\mathbf{A}\mathbf{x} - \mathbf{b}\|_2^2 \quad \text{subject to } x \geq 0,$$

with the attraction of being differentiable and convex, penalizing dose volumes that exceed a doctor's prescribed constraint. The Lagrangian becomes

$$L(\mathbf{x}, \boldsymbol{\lambda}) = \min \frac{1}{2} \|\mathbf{A}\mathbf{x} - \mathbf{b}\|_2^2 - \boldsymbol{\lambda}^T \mathbf{x}.$$

The above problem can be solved with dual gradient descent (DGD), but DGD has the drawback that the primal and dual updates are not robust to objective's constraints [25]. The alternating direction method of multipliers (ADMM) [25] tackles the robustness problem by adding a quadratic penalty term to the Lagrangian and alternately updating the \mathbf{x} and $\boldsymbol{\lambda}$ variables in a "broadcast and gather" process. This turns out to be attractive since we will be solving a large-scale learning problem for the optimal beam angle set combination. Introducing an auxiliary variable \mathbf{z} , the above is transformed into the following

$$\min_{\mathbf{x}} \frac{1}{2} \|\mathbf{A}\mathbf{x} - \mathbf{b}\|_2^2, \quad \text{subject to } \mathbf{z} = \mathbf{x}, \mathbf{z} \geq 0.$$

so that the Lagrangian can be written as,

$$\min_{\mathbf{x}, \mathbf{z}} \frac{1}{2} \|\mathbf{A}\mathbf{x} - \mathbf{b}\|_2^2 - \boldsymbol{\lambda}^T (\mathbf{z} - \mathbf{x}) + \frac{\rho}{2} \|\mathbf{z} - \mathbf{x}\|_2^2, \quad (2)$$

where $\boldsymbol{\lambda} \in \mathbb{R}^n$ is a multiplier and $\rho > 0$ is an ADMM penalty parameter. The \mathbf{x} subproblem to (2) yields

$$\min_{\mathbf{x}} \frac{1}{2} \mathbf{x}^T (\mathbf{A}^T \mathbf{A} + \rho \mathbf{I}) \mathbf{x} + (\boldsymbol{\lambda}^T - \mathbf{A}^T \mathbf{b} - \rho \mathbf{z}^T) \mathbf{x},$$

so that the \mathbf{x} -update (due to the convex quadratic nature of the problem) becomes,

$$\mathbf{x}^{k+1} = (\mathbf{A}^T \mathbf{A} + \rho \mathbf{I})^{-1} (\mathbf{A}^T \mathbf{b} + \rho \mathbf{z}^k - \boldsymbol{\lambda}^k). \quad (3)$$

Similarly, the \mathbf{z} -update for (2) can be found by the \mathbf{z} -minimization subproblem

$$\min_{\mathbf{z}} -\boldsymbol{\lambda}^T \mathbf{z} + \frac{\rho}{2} \|\mathbf{z} - \mathbf{x}\|_2^2 := \min_{\mathbf{z}} \frac{\rho}{2} \|\mathbf{z} - \mathbf{x} - \frac{1}{\rho} (\boldsymbol{\lambda})\|_2^2.$$

Using the soft-thresholding operator, $S_{\lambda/\rho}$, we find that

$$\mathbf{z}^{k+1} = S_{\lambda/\rho}(\mathbf{x}^{k+1} + \boldsymbol{\lambda}^k), \quad (4)$$

where $S_{\lambda/\rho}(\tau) = (x - \lambda/\rho)_+ - (-\tau - \lambda/\rho)_+$. $\boldsymbol{\lambda}$ is updated as

$$\boldsymbol{\lambda}^{k+1} = \boldsymbol{\lambda}^k - \gamma(\mathbf{z}^{k+1} - \mathbf{x}^{k+1}), \quad (5)$$

where γ is a parameter that controls the step length. The inverse operation in (3) can be carried out with any iterative solver e.g. conjugate gradient. We use an over-relaxation parameter, $\alpha^k = 1.5$, and set the quadratic penalty to $\rho = 1.5$, in the \mathbf{z} and $\boldsymbol{\lambda}$ updates: $\alpha^k \mathbf{A} \mathbf{x}^{k+1} - (1 - \alpha^k) \mathbf{z}^k$. The stopping criterion is met when the primal and dual residuals are sufficiently small, *i.e.* ,

$$r^k = \|\mathbf{x}^k - \mathbf{z}^k\|_2 \leq \epsilon^{\text{pri}} \quad \text{and} \quad s^k = \|\rho(\mathbf{z}^{k+1} - \mathbf{z}^k)\|_2 \leq \epsilon^{\text{dual}},$$

with,

$$\epsilon^{\text{pri}} = \sqrt{\rho} \epsilon^{\text{abs}} + \epsilon^{\text{rel}} \max\{\|\mathbf{x}^k\|_2, \|\mathbf{z}^k\|_2\}, \quad \text{and}$$

$$\epsilon^{\text{dual}} = \sqrt{n} \epsilon^{\text{abs}} + \epsilon^{\text{rel}}(\rho \boldsymbol{\lambda}^k),$$

where $\epsilon^{\text{pri}} > 0$, $\epsilon^{\text{dual}} > 0$ are the primal and dual feasibility tolerances for the primal and dual feasibility conditions (see [25, §3.3]). We set $\epsilon^{\text{abs}} = 10^{-4}$ and $\epsilon^{\text{rel}} = 10^{-2}$.

2.6 Game Tree Simulation

Consider b^d possible move sequences for state, s_t of a gantry-patient setup where b is the beam angles chosen to construct a fluence and d is the total number of discretized gantry beam angles. For $b = 180$ and $d = 5$, for example, we have 180^5 possible search directions. This renders exhaustive search infeasible. We therefore leverage on Monte Carlo simulations, encouraged by their recent success in large games e.g. [26–28], by combining traditional min-max evaluation of a tree’s leaves with Monte Carlo simulations. We iteratively run random simulations from a tree’s root node through its sub-nodes, randomly choosing actions, while a back-up operator progressively averages the outcome of many random simulations to min-max as the amount of simulation expands, until we arrive at a terminal state. For a state s_t other than the root node, s_0 , an **expansion policy** decides whether to recursively **expand** the current state, executing actions $\{a_0, \dots, a_t\}$, or if it should roll out the current game to completion.

During each expansion process (see Algorithm 1), the reward or cost of a child node is computed by taking the optimal fluence cost posed in (1), and the computed node is appended to the tree only if it does not exist in the tree already. At each MDP episodic setting, many games of self-play are unrolled from the tree’s root node, s_0 until a terminal leaf is reached. We compute the mean outcome of every simulation through state s in which action a is selected, *i.e.* the tree’s $Q(s, a)$ -value, as $Q(s, a) = \frac{1}{N(s, a)} \sum_{i=1}^{n(s)} I_i(s, a) \zeta_i$ where $N(s, a) = \sum_{i=1}^{n(s)} I_i(s, a)$ is the total number of simulations in which action a was selected in state s , $n(s)$ is the total number of times

a game is played through state s , and ζ_i is the outcome of the i th simulation played out from s . Specifically,

$$I_i(s, a) = \begin{cases} 1, & \text{if } a \text{ was selected on the } i\text{'th policy rollout} \\ 0, & \text{otherwise.} \end{cases}$$

During simulations, each state and action in the search tree are updated as follows $n(s_t) \leftarrow n(s_t) + 1$; $N(s_t, a_t) \leftarrow N(s_t, a_t) + 1$; $Q(s_t, a_t) \leftarrow Q(s_t, a_t) + r(s_t, a_t)$, where $r(s_t, a_t)$ is the reward given to the agent after action a is executed while transitioning from state s_t to s_{t+1} . This MCTS implementation makes beam angle transitions evolve in a highly selective, best-first behavior – expanding promising areas of the search space in deeper, given infinite memory and computation.

Our tree-search implements a sparse look-ahead strategy for large state-space MDPs in a **perfect recall** game, *i.e.* each node’s current information state implies knowledge of their direct ancestral nodes. It is a sequential simulation of different beam angle combinations whose transitions are governed by probabilities obtained from a two-player zero-sum game of neural fictitious self-play (FSP). A neural network roll-out policy guides the search for a *best-first* beam angle set. The best-first leaf node encountered is given by the child node with the highest reward along a tree that is expanded.

We randomly sample beam angles within the gantry angle space by carrying out a lookahead search at fixed depth; we restrict sampling to 90 discretized grid in Θ at every stage of our simulation. A partial tree of beam angle candidates is randomly constructed, starting from a root node, and we progressively add child nodes to the current node in a **selection** process guided by move probabilities, $p(s, a)$. At the first iteration, the subset of beam angles are randomly sampled from Θ . In our expansion phase (see algorithm 1), to prevent angles from being too close to one another, we define a minimum pairwise distance, $\bar{d}_i \in \mathbb{R}^+$ between the beamlets in a beam block, given by $\|\theta_i - \theta_j\| \geq \bar{d}_i, \forall \{j \in m \setminus i\}$ where we set $\bar{d}_i = 20$. By repeatedly performing roll-outs, we maintain a history of state-action value pairs, stored along the edges of the tree. This aids faster convergence if the same state is encountered more than once: we can bias an action selection based on old actions that were chosen.

When we finish each simulation, a ‘best move’ for the current beam block is selected, as computed by the tree search; we exponentiate the move probabilities by a temperature slightly larger than unity to encourage diversity in early play; specifically, we compute

$$p(a|s_0; \psi) = \frac{N(s_0, a)^{1/\tau}}{\sum_b N(s, b)^{1/\tau}},$$

where τ is the temperature factor that diversifies the move probabilities. The UCT [7] algorithm applied to optimal beam angle selection is presented in algorithm 1.

Definition 3. A minimizer player is at a **terminal state** if the FMO cost for the beams at a leaf node is greater than the cost of the beams at its direct ancestor node.

Definition 4. A maximizer player has reached a **terminal state** if the FMO cost for the beams at a leaf node is less than the FMO cost for the beams at its direct ancestor node.

Algorithm 1 Deep BOO Monte Carlo Tree Search

```

function MCTS( $s_0$ )
   $s_0 \leftarrow \mathbf{x}_0(s_0)$ 
  while search time < budget do
     $\bar{x} \leftarrow \text{EXPAND\_POLICY}(\mathbf{x}_0)$ 
     $\bar{x}.r \leftarrow \text{FMO\_POLICY}$ 
    BACKUP( $\bar{x}, \bar{x}.r$ )
  end while
  return BEST_CHILD( $\mathbf{x}_0, c$ )
end function

function SELECT_MOVE( $x, c$ )
  if  $p_1$  to play then
    return  $\arg\max_{\bar{x} \in \text{children of } x} Q(\bar{x}) +$ 
     $c\sqrt{\frac{2 \ln n(\bar{x}.s)}{N(\bar{x}.s, a)}}$ 
  else
    return  $\arg\min_{\bar{x} \in \text{children of } x} Q(\bar{x}) -$ 
     $c\sqrt{\frac{2 \ln n(\bar{x}.s)}{N(\bar{x}.s, a)}}$ 
  end if
end function

function EXPAND_POLICY( $x$ )
  while  $x$  is nonterminal do
    if  $x$  is not fully expanded then
      return EXPAND( $x$ )
    else
       $x \leftarrow \text{BEST\_CHILD}(x, c)$ 
    end if
  end while
  return  $x$ 
end function

function FULLY_EXPANDED( $x, d$ )
   $d_i \leftarrow \text{pairwise\_distance}(x.s)$ 
   $\text{min\_elem} \leftarrow \min(d)$ 
  if  $\text{min\_elem} < d$  then
    return True
  else

```

```

    return False
  end if
end function

function FMO_POLICY( $x$ )
  find optimal fluence objective,
   $h^*(x(s)|\cdot)$ 
  return  $r = -h^*(x(s)|\cdot)$ 
end function

function EXPAND( $x$ )
  sample a  $\bar{\theta}$  using prior  $x.p(s, a)$ 
   $\bar{a} = \text{SELECT\_MOVE}(x, c)$ 
  add  $\bar{a}$  to tried actions  $\bar{\mathcal{A}}$ 
  form new node  $\bar{x}.\bar{s}$ 
  with  $\bar{\theta} \leftarrow \bar{\theta} + \bar{a}$ 
  with  $\pi_{t-1}$ , create  $\bar{x}.p(\bar{s}, \bar{a}), \bar{x}.\bar{v}(\cdot)$ 
  while not  $\bar{x}$  in children of  $x_0$  do
    add child  $\bar{x}$  to  $x$ 
  end while
  return  $\bar{x}$ 
end function

function BACK_UP( $x, c$ )
  while  $\bar{x}$  is not null do
     $N(\bar{x}) \leftarrow \bar{x} + 1$ 
     $Q(\bar{x}) \leftarrow Q(\bar{x}) + \bar{x}.r$ 
     $\bar{x} = \text{parent of } \bar{x}$ 
  end while
end function

function BEST_CHILD( $x_0$ )
  if  $p_1$  to play then
    return  $x_0[\arg\min \text{ children of } x_0.r]$ 
  else
    return  $x_0[\arg\max \text{ children of } x_0.r]$ 
  end if
end function

```

Definitions § 3 and § 4 help preserve the neighborhood search for the beam improvement tuning as specified earlier. When angles are at the edges *i.e.* 0° or 360° and an angle change outside the range $0 \leq \theta \leq 360$ is recommended, we “wrap” around to enforce cyclicity. The index of the angle to select is determined by taking an argmax of the mixed strategy produced by the tree policy $\pi_{\psi_{t-1}}$; this policy is constantly being optimized in a separate thread. Similarly, the direction in which to modify the angle is determined by an argmax of the third head of the tree policy $\pi_{\psi_{t-1}}$ as discussed in § 2.4. The **EXPAND_POLICY** and **FMO_POLICY** procedures of the MCTS simulation in algorithm 1 can be seen as a form of Add/Drop simulated annealing as described in [3]. The **BEST_CHILD** procedure compares the quality of all beam angle sets traversed as the root node is expanded to one or more child nodes; the greedy approach of selecting the beam angle set with the highest reward results in a locally optimal set of beam angles candidates at each iteration of running a game.

Definition 5. We define an **upper confidence bound**, $U(s, a)$, on $Q(s, a)$ that adds an exploration bonus that is highest for seldomly visited state-action pairs so that the tree expansion policy selects the action a^* that maximizes the augmented value:

$$\bar{Q}(s, a) = Q_j(s, a) + c \sqrt{\frac{2 \ln n(s)}{N(s, a)}}, \quad \text{where } a^* = \arg \max_a \bar{Q}(s, a). \quad (6)$$

$Q(s, a)$ is the highest average observed reward from node j – encouraging exploitation of the current node, and $\ln n(s)$ is the natural logarithm of the total number of roll-outs through state s . The second term in (6) encourages exploration of other beam angles and c is a scalar exploration constant. Note that (6) is a version of the **UCB1** algorithm [7]. This estimates the expected reward of a set of beam candidates once we compute its upper confidence.

2.7 Self-Play Neuro-Dynamic Programming

This section describes the approximate dynamic programming scheme and self-play formulation for generating saddle point equilibrium strategies for an *approximately* optimal outcome (value) by playing a weakened fictitious self-play (FSP) between two neural network behavior strategies. We consider a trial-and-error search problem via interaction with the dynamical system so as to discover a mapping between poatient geometry and beam angles in order to maximize an extrinsic reward signal; we approach this with optimal control of incompletely known **Markov decision processes** (MDP). The MDP consists of states \mathcal{S} , actions, \mathcal{A} , a transition probability, $\mathcal{P}_{ss'}^a$, and a reward function \mathcal{R}_s^a . $\mathcal{P}_{ss'}^a$ is a probability distribution that governs the evolution of states e.g. from $s \rightarrow s'$, while \mathcal{R}_s^a determines a reward after the transitions occur. In **Q-learning**, an agent’s experience is made up of distinct episodes: at the t ’th episode, the agent observes its current state, s_t , selects and executes an action a_t , which transitions the agent to a new state s_{t+1} ; an immediate reward, r_t , is subsequently given to the agent, by which the previous Q-values are adjusted. Q-learning relies on *value iteration* to reach convergence. In practice, this takes a long time to complete. **Batch Q-learning** algorithms e.g. [29] attempt to learn a stochastic policy $\pi_\psi : \mathcal{S} \times \mathcal{A} \rightarrow \mathcal{R}$ that maximizes the cumulative discounted reward $\sum_{t=0}^{T-1} \gamma^t r(s_t, a_t)$, where ψ are the parameters of a policy.

Weakened fictitious self-play applies machine learning to determine an *approximate* best response strategy to an opponent’s mixed strategy in games of self-play. An agent continually plays a game against an opponent and the outcome of the game is given by averaging the outcome of all individual plays.

We apply FSP in a machine learning framework to a game’s strategy profile so that each player plays an *approximate* best response strategy to their opponent’s mixed strategy at each iteration. In our formulation, each player does not necessarily know the strategy of its opponent ahead of time *i.e.* their security levels do not necessarily coincide. To ensure that equilibrium can be found within pure strategies, we let one player act after observing the decision outcome of the other player. The game thus has a **dynamic** property since the strategy of the successive acting player explicitly depends on that of the first player [30, pp.22].

Each player’s action is governed by a mixed strategy – obtained by adding a Gaussian random walk sequence with standard deviation 2 to the prior probability distribution predicted by the neural network policy or computed by the tree policy; this is then normalized by the sum of the resulting noised distribution. We do this to encourage further exploration and to transform each player’s pure strategy to a mixed strategy. As such, a player’s mixed strategy is simply a random variable whose values are the player’s pure strategies. Players p_1 , and p_2 ’s mixed strategies are independent random variables, repeatedly implemented during game simulations such that their actual decisions are based on chance events. However, as the number of times the game is played gets larger, the frequency with which different actions for p_1 and p_2 are chosen will converge to the probability distribution that characterize their random strategies [30, pp.24]. For a game Γ , suppose that $y = \{y_1, \dots, y_m \mid \sum_{i=1}^m y_i = 1\}$ and $z = \{z_1, \dots, z_n \mid \sum_{i=1}^n z_i = 1\}$ are the respective probability distributions for players p_1 and p_2 , defined on the n and m –dimensional simplices respectively, the average value of the game will correspond to player p_1 minimizing a cost $\mathcal{J}(y, z) = y^T \Gamma z$ and player p_2 maximizing $\mathcal{J}(y, z)$.

The fictitious self-player samples from previous episodes of the game of self-play at each iteration k . For each **pure strategy**, $p(s, a)$, predicted by the neural network policy, f_ψ , each player makes a decision governed by a probability distribution on the space of its pure strategies. The opposing agent’s policy is randomly sampled from a previous checkpoint of the training scheme. The goal of the two-player zero-sum neural fictitious self-play is to drive the network to an approximate saddle equilibrium, via experiential learning, thus guaranteeing that the realization of an approximate optimal value function for the optimal beam angle set that generates a desired fluence/DVH profile.

3 Conclusion

Beam orientation optimization is a key component of conformal IMRT radiotherapy TPS. It has a nonconvex solution surface given the way the dose coefficients can significantly alter based on the gantry angle from which beams are aimed to a target volume. As such, in modern clinics, this problem is typically solved with many hours of planning, hand-tuning and refinement – usually by experienced dosimetrists and radiation therapists.

Given the long time traditional optimization approaches take in solving this problem, we adopt a hybrid approach, leveraging on monte carlo simulation of games in high

dimensional state-spaces, neuro-dynamic programming, convex optimization of fluence profiles of a target radiation, and game theory to arrive at good candidate beamlets. Our monte carlo tree search formulation is the first, to the best of our knowledge, that transforms the BOO problem into a monte carlo tree search strategy; and provides a pseudocode that shows how we implement the tree search to navigate the complex state space of respective beamlets. In the part II of this paper, we elucidate on the end-to-end optimization pipeline and provide our initial results based on a set of numerical simulations for select anonymized patients data in our clinic.

References

1. Craft, D.: Local beam angle optimization with linear programming and gradient search. *Physics in Medicine & Biology* **52**(7), N127 (2007) [2](#), [3](#)
2. Söderström, S., Brahme, A.: Optimization of the Dose Delivery In A Few Field Techniques Using Radiobiological Objective Functions. *Medical physics* **20**(4), 1201–1210 (1993) [2](#)
3. Aleman, D.M., Kumar, A., Ahuja, R.K., Romeijn, H.E., Dempsey, J.F.: Neighborhood Search Approaches to Beam Orientation Optimization in Intensity Modulated Radiation Therapy Treatment Planning. *Journal of Global Optimization* **42**(4), 587–607 (2008) [2](#), [3](#), [13](#)
4. LeCun, Y., Bengio, Y., Hinton, G.: Deep Learning. *Nature* **521**(7553), 436–444 (2015) [2](#)
5. Gelly, S., Silver, D.: Monte-Carlo tree search and rapid action value estimation in computer Go. *Artificial Intelligence* **175**, 1856–1875 (2011) [2](#)
6. Coulom, R.: Efficient Selectivity and Backup Operators in Monte-Carlo Tree Search. *International Conference on Computers and Games* (2006) [2](#)
7. Kocsis, L., Szepesvári, C.: Bandit based Monte-Carlo Planning. *European Conference on Machine Learning* (2006) [2](#), [11](#), [13](#)
8. Ogunmolu, O., Gans, N., Summers, T.: Minimax Iterative Dynamic Game : Application to Nonlinear Robot Control. *IEEE International Conference on Intelligent Robots and Systems* (2018) [2](#)
9. Heinrich, J., Lanctot, M., Silver, D.: Fictitious self-play in extensive-form games. In: *International Conference on Machine Learning*, pp. 805–813 (2015) [3](#)
10. Bertsimas, D., Cacchiani, V., Craft, D., Nohadani, O.: A Hybrid Approach To Beam Angle Optimization In Intensity-modulated Radiation Therapy. *Computers & Operations Research* **40**(9), 2187–2197 (2013) [3](#)
11. Jia, X., Men, C., Lou, Y., Jiang, S.B.: Beam Orientation Optimization For Intensity Modulated Radiation Therapy Using Adaptive L2,1-minimization. *Physics in Medicine and Biology* **56**(19), 6205–6222 (2011) [3](#)
12. Bortfeld, T., Schlegel, W.: Optimization of beam orientations in radiation therapy: Some theoretical considerations. *Physics in Medicine & Biology* **38**(2), 291 (1993) [3](#)
13. Djajaputra, D., Wu, Q., Wu, Y., Mohan, R.: Algorithm and Performance Of A Clinical Imrt Beam-angle Optimization System. *Physics in Medicine & Biology* **48**(19), 3191 (2003) [3](#)
14. Pugachev, A., Xing, L.: Computer-assisted selection of coplanar beam orientations in intensity-modulated radiation therapy. *Physics in Medicine & Biology* **46**(9), 2467 (2001) [3](#)
15. Wang, C., Dai, J., Hu, Y.: Optimization of beam orientations and beam weights for conformal radiotherapy using mixed integer programming. *Physics in Medicine & Biology* **48**(24), 4065 (2003) [3](#)
16. Lim, G.J., Ferris, M.C., Wright, S.J., Shepard, D.M., Earl, M.A.: An optimization framework for conformal radiation treatment planning. *INFORMS Journal on Computing* **19**(3), 366–380 (2007) [3](#)

17. D D'Souza, W., Meyer, R.R., Shi, L.: Selection of beam orientations in intensity-modulated radiation therapy using single-beam indices and integer programming. *Physics in Medicine & Biology* **49**(15), 3465 (2004) [3](#)
18. Hou, Q., Wang, J., Chen, Y., Galvin, J.M.: Beam orientation optimization for imrt by a hybrid method of the genetic algorithm and the simulated dynamics. *Medical Physics* **30**(9), 2360–2367 (2003) [3](#)
19. Huang, G., Liu, Z., Weinberger, K.Q., van der Maaten, L.: Densely Connected Convolutional Networks. *arXiv preprint arXiv:1608.06993* (2016) [4](#)
20. He, K., Zhang, X., Ren, S., Sun, J.: Deep Residual Learning For Image Recognition. In: *Proceedings of the IEEE conference on computer vision and pattern recognition*, pp. 770–778 (2016) [4](#), [6](#)
21. Agrawal, R.: Sample mean based index policies by $o(\log n)$ regret for the multi-armed bandit problem. *Advances in Applied Probability* **27**(4), 1054–1078 (1995) [4](#)
22. Ioffe, S., Szegedy, C.: Batch Normalization: Accelerating Deep Network Training By Reducing Internal Covariate Shift. *arXiv preprint arXiv:1502.03167* (2015) [7](#)
23. Hahnloser, R.H., Sarpeshkar, R., Mahowald, M.A., Douglas, R.J., Seung, H.S.: Digital selection and analogue amplification coexist in a cortex-inspired silicon circuit. *Nature* **405**(6789), 947 (2000) [7](#)
24. He, K., Zhang, X., Ren, S., Sun, J.: Delving Deep into Rectifiers: Surpassing Human-level Performance on Imagenet Classification. In: *Proceedings of the IEEE international conference on computer vision*, pp. 1026–1034 (2015) [8](#)
25. Boyd, S., Parikh, N., Chu, E., Peleato, B., Eckstein, J.: Distributed Optimization and Statistical Learning via the Alternating Direction Method of Multipliers. *Foundations and Trends in Machine learning* **3**(1), 1–122 (2011) [9](#), [10](#)
26. Chung, M., Buro, M., Schaeffer, J.: Monte carlo planning in rts games. In: *CIG*. Citeseer (2005) [10](#)
27. Silver, D., Huang, A., Maddison, C.J., Guez, A., Sifre, L., Van Den Driessche, G., Schrittwieser, J., Antonoglou, I., Panneershelvam, V., Lanctot, M., Dieleman, S., Grewe, D., Nham, J., Kalchbrenner, N., Sutskever, I., Lillicrap, T., Leach, M., Kavukcuoglu, K., Graepel, T., Hassabis, D.: Mastering the game of Go with deep neural networks and tree search. *nature* **529**, no. 7587: 484–489. (2016) [10](#)
28. Silver, D., Schrittwieser, J., Simonyan, K., Antonoglou, I., Huang, A., Guez, A., Hubert, T., Baker, L., Lai, M., Bolton, A., et al.: Mastering the Game Of Go Without Human Knowledge. *Nature* **550**(7676), 354 (2017) [10](#)
29. Mnih, V., Kavukcuoglu, K., Silver, D., Rusu, A.a., Veness, J., Bellemare, M.G., Graves, A., Riedmiller, M., Fidjeland, A.K., Ostrovski, G., Petersen, S., Beattie, C., Sadik, A., Antonoglou, I., King, H., Kumaran, D., Wierstra, D., Legg, S., Hassabis, D.: Human-level Control Through Deep Reinforcement Learning. *Nature* (7540), 529–533 (2015). DOI 10.1038/nature14236 [13](#)
30. Basar, T., Olsder, G.J.: Dynamic noncooperative game theory, vol. 23. Siam (1999) [14](#)